# PROCEEDINGS OF SPIE

SPIEDigitalLibrary.org/conference-proceedings-of-spie

Three-dimensional surface reconstruction of the papilla nervi optici using scanning laser ophthalmoscopic sequences

Altmann, Markus, Herpers, Rainer, Kuenzer, Isabel, Englmeier, Karl-Hans

Markus Altmann, Rainer Herpers, Isabel Kuenzer, Karl-Hans Englmeier, "Three-dimensional surface reconstruction of the papilla nervi optici using scanning laser ophthalmoscopic sequences," Proc. SPIE 2434, Medical Imaging 1995: Image Processing, (12 May 1995); doi: 10.1117/12.208705



Event: Medical Imaging 1995, 1995, San Diego, CA, United States

# 3D surface reconstruction of the Papilla Nervi Optici using Scanning Laser Ophthalmoscope sequences

Markus Altmann, Rainer Herpers, Isabel Künzer, Karl-Hans Englmeier

GSF-Forschungszentrum für Umwelt und Gesundheit, Institut für Medizinische Informatik und Systemforschung\* Neuherberg, Ingolstädter Landstr. 1, D-85764 Oberschleißheim, Germany

#### **ABSTRACT**

A method of a three-dimensional surface reconstruction of the retina in the area of the papilla is presented. The surface reconstruction is based on a sequence of discrete gray-level images of the retina recorded by a Scanning Laser Ophthalmoscope (SLO). The underlying assumption of the developed surface reconstruction algorithm is that the depth information is also encoded in the brightness values of the single pixels beside the ordinary spatial 2D information. The brightness of an image position depends also on the degree of reflection of a confocal laser beam. Only these surface structures produce a high response of the focused laser light, which are located directly in the focus plane of the confocal laser beam. The occurring disparities between the single images of a sequence are considered to be approximately linear and are corrected by applying the cepstrum technique. The depth information is estimated out of the volumetric representation of the image sequence by searching the maximal value of the brightness within a computed depth profile at every image position. In the resulting range images disturbances which occur during the recording cause wrong local estimations of the depth information. These local disturbances are corrected by applying especially developed surface improvement processes. The work is completed by investigating several different approaches to reduce the noisy and disturbances of SLO image data.

## 1. INTRODUCTION

Changes of the volume and morphology of the Papilla Nervi Optici (blind spot), subsequently called papilla, can be found at diseases with raised intraocular pressure. A hypertension or high blood pressure with a continuous raising of the blood pressure of values greater than 140 mmHg systolic and greater than 90 mmHg diastolic causes irreversible damages of the retina. This retinopathia often goes along with an oedema of the papilla [8]. All other space requiring processes like the growth of small tumors with the compression of the optic nerve also cause changes of the structure of the papilla [6].

For an early recognition or diagnosis of this ophmopathia a 3D reconstruction of the papilla could be very helpful. By the application of this method, changes of the morphology of the papilla and its surroundings can early be detected comparing different investigations. So the diagnosis and the therapy may be improved.

The confocal laser beam of the Scanning Laser Ophthalmoscope (SLO) scans an object focused relatively to a fixed area called focus depth or focus plane [9] (Fig. 1). During scanning only those structures of the eye ground which are exactly located in the focus plane reflect optimally the confocal laser beam. Moreover, the confocal laser beam at those locations will be reflected substantially stronger than at areas before or behind the actual focus depth. Therefore, the recorded SLO images also contain depth information beside the 2D information. Within the gray-level images recorded at different but certain focus planes, bright structures, i. e., image parts with high gray-level values, finally correspond to those eye ground structures which are exactly located in the focused plane.



Fig. 1: Extracts of a SLO recording sequence in the range of the papilla from a focus depth of +0.2 dpt (upper left) up to -1.5 dpt (lower right) with increasing degree of saturation in the bottom of the papilla.

<sup>\*</sup>Correspondance to: Rainer Herpers, Isabel Künzer, GSF Medis-Institut, D-85764 Oberschleißheim, E-mail: herpers, kuenzer@gsf.de,

Therefore, these bright structures indicate the relation of a surface boundary to the considered focus depth and are called "relevant" in the following. Figure 2 shows typical examples out of a SLO sequence with marked bright structures which are located near the used focus depth. While the depth information is encoded in the gray-level values of each pixel position, the brightness represents the distance between the surface boundary and the focused plane of the confocal laser beam.

The presented reconstruction method of the surface structure is based on the brightness information of these slice images recorded by a Scanning Laser Ophthalmoscope (SLO). The records are 8-bit gray-level images of the size of 1024x512 pixels. The useable image information encloses an area of about 700x450 pixels or less because of image borders and included descriptions. The focus depth varies stepwise in distances of 0.05 dpt from -1.5 dpt up to +0.2 dpt with a total investigation time of about five minutes for the whole sequence. A sequence of 32 images (slices) is scanned within this range during one investigation. To reduce the computing cost of the surface reconstruction only the region of interest (ROI) containing the papilla and its surroundings is extracted out of all images (Fig. 1).

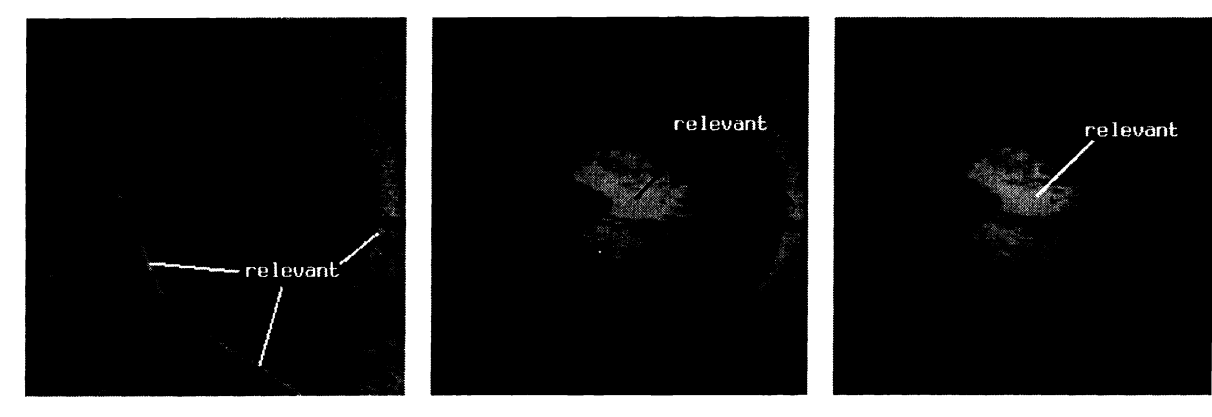


Fig. 2: The first (at +0.2 dpt), the middle (at -0.55 dpt) and the last slice (at -1.5 dpt) of a SLO-sequence of 32 records are shown. These images represent focus planes with decreasing distances to the Papilla from left to right. The brighter areas within the images are relevant surface positions for the following surface reconstruction.

After the short introduction of the basics of the Scanning Laser Ophthalmoscope (SLO) data generation an approach to correct the occurring disparities is presented. The investigated Cepstrum technique is introduced for the one dimensional case, then it is described for two dimensions and at least the adaptation of the Cepstrum to the SLO data is presented. The different steps of the developed surface reconstruction method are described in chapter 3 and 4. Some possibilities to optimize the reconstruction method by using a replacement-tolerance or applying a recursive proceeding are presented at the end of the paper.

#### 2. DISPARITY CORRECTION

It is necessary to remove the disparities which may occur in X- and Y-direction between the single slices of the image sequence before a reconstruction of the surface can be computed. The disparities are not avoidable, because there are minor delays up to 1 sec. for storing the image data from one image to the next. The reason is that the patient is not able to keep absolutely still his eyes during the whole recording time. Due to these shifts of corresponding image structures in one sequence it is not possible to build an errorless 3D volume of the image data. Since these disparities are small compared to the size of the whole images, they are considered to be approximately linear. Therefore, the contained complex disparities are only considered as linear shifts in X- and Y-direction. Assuming a linear displacement of the image structures in X- and Y-direction, the amount and the direction of the displacements from one image to the next can be calculated by applying the Power Cepstrum [2], subsequently called cepstrum.

# 2.1. Theory of the cepstrum technique for one dimension

The cepstrum was first described as an heuristic method to determine the echo response time in one dimensional, composed seismographic signals by Bogert et al. [1]. One of the major properties of this method is the applicability to disturbed and noisy signals. The cepstrum of a function g(x) is defined as the power spectrum of the logarithm of the power spectrum of that function [5]: Cepstrum  $\{g(x)\} = \|\mathcal{F}\{\log(\|\mathcal{F}\{g(x)\}\|^2)\}\|^2$ , where  $\mathcal{F}\{.\}$  represents the Fourier transform.

<sup>&</sup>lt;sup>1</sup>an anagram of the word spectrum

The delay echo of an 1D signal becomes manifest as cosine wave in the logarithm of its power spectrum. The frequency of this wave is determined by the power spectrum of the logarithm of its spectrum. A peak at the period time of the cosine wave appears in its power spectrum. Since the logarithm of the spectrum is a function of the frequency, so the unit of the frequency of this cosine wave is oscillation per oscillation per time, i. e. the time itself [1]. Therefore, the unit of the abscissa in the cepstrum is the time unit, too. So the echo response time can easily be determined by detecting the time of the first peak in the cepstrum signal. This method is extended to 2D signals or image data to calculate spatial displacements of two corresponding images [10].

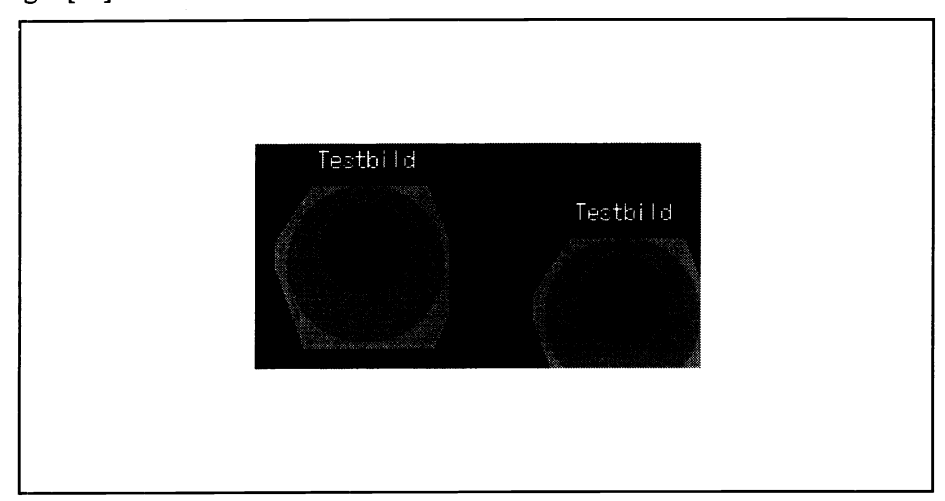


Fig. 3: Attachment of a test image (D=128) with its corresponding shifted (x=20, y=30) image in a 4Dx2D-window as used as input signal for the 2D power cepstrum.

## 2.2. Cepstrum technique for 2D image data

In the digital image processing the cepstrum is used as a method to detect the direction and the amount of linear shifts of image structures between two different images of one object [10]. For the application of the cepstrum the two images, for which the shift has to be determined, are attached to each other and inserted into a surrounding window. Figure 3 shows this attachment for a shifted test image of size D = 128. Due to the application of the FFT with the cepstrum, all image sizes D are expressed in powers of two. The size of the surrounding window is 4Dx2D. By this attachment a horizontal shift D (image width) is included in the shift to be determined, which has to be taken into account at the calculation of the result [5, 10]. The application of the cepstrum to a signal  $f(x, y) = s(x, y) + s(x - x_0, y - y_0)$  which is composed of two identical parts where one is only shifted by  $(x_0, y_0)$  yields:

Cepstrum
$$\{f(x,y)\}\ = Cepstrum\{s(x,y)\} + \sum_{n=-\infty}^{\infty} \frac{\delta(x-n\cdot x_0, y-n\cdot y_0)}{n}$$

i. e. there is a strong component in the resulting signal exactly located at the site of the shift  $(x_0, y_0)$ . The principle of the cepstrum technique applied to 2D data is shown in Figures 3 and 4 with a test image.

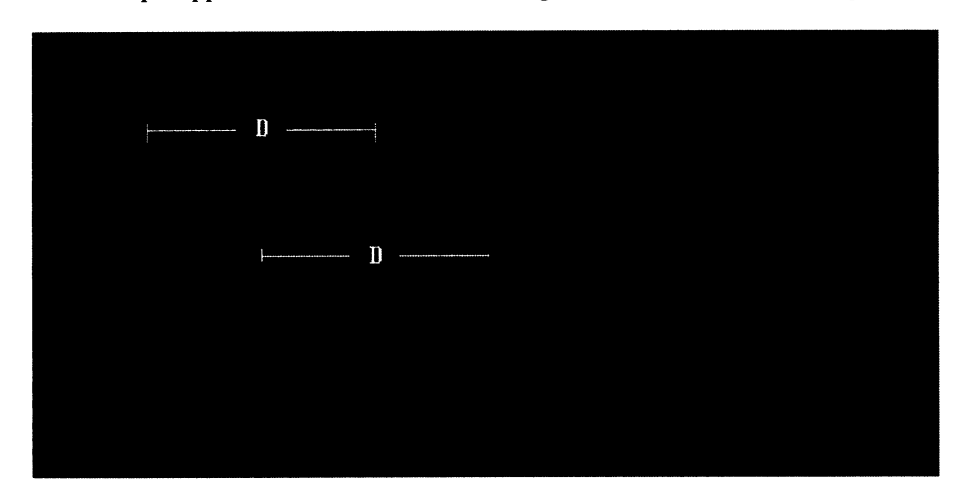


Fig. 4:
Cepstrum signal of Fig. 3 with the area marked to which the search for the peak caused by the shift can be restricted. In the middle of the two circles the resulting peaks are shown. They are located mirrored by the origin.

After the application of the cepstrum two peaks can be detected mirrored by the origin (Fig. 4). While the amount of the shift to be determined is well expressed and the artificial shift D caused by the included attachment the resulting peak signal is differs enough from the zero frequency. The searched peak position for the disparity correction can now easily be determined using a maximum search algorithm. The maximum search, however, can be restricted to the range of D/2 up to 3D/2 because of the known shift D [10]. By insertion of two DxD images in a surrounding window of a size of 4Dx2D the maximum search can be carried out in a continuous region from D/2 to 3D/2 referred to the origin located in the center of the resulting 2D signal. The known zero shift D has to be subtracted from the determined coordinates of the maximum in the considered region to get the shift vector to be detected of the image at the end of the calculation.

## 2.3. Cepstrum applied to SLO images

Only image parts of a size of DxD pixels (in this case: D = 256) at a fixed central position are selected to determine the disparities of all slices of a sequence. These image parts should contain the structure of the papilla but this is not strictly necessary for the displacement detection. Due to the insensitivity to noise of the cepstrum algorithm a preprocessing of the images with a filter is not necessary. While the disparity correction algorithm can only be calculated for two slices of an image sequence which are directly neighboured, the disparity correction of the whole image sequence has to be computed sequentially from one image to its neighbour.

While attaching two neighboured SLO images an artificial vertical shift  $D_y$  is also added to the secondary image. This is necessary to move the signal of the shift out of the area of the zero frequencies of the cepstrum, because the amount of the shift may often be very small or zero. The expected signal of the included disparity would be hidden by the cepstrum signal itself without an additional vertical shift.

Applying this method to all neighbouring image pairs of a sequence, the shift vectors which are needed can sequentially be calculated. Then the resulting vectors are added from one image to the next to determine the summed shift relative to a reference image. Figure 5 shows two examples of an image pair out of a SLO sequence before and after the disparity correction.

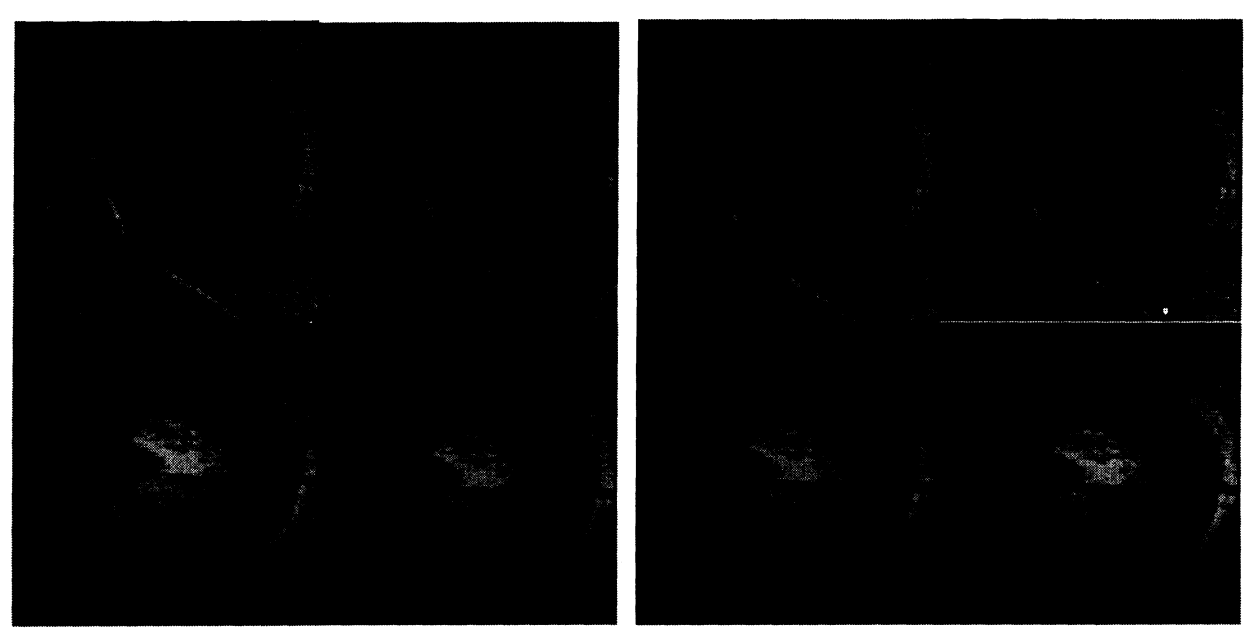


Fig. 5: Pairs of two neighboured SLO images, on the left before the disparity correction by the cepstrum, on the right after application of the cepstrum and shifting by the detected vector. In the upper line a sample out of the beginning of the sequence is shown, in the lower line a sample out of the end of the sequence.

## 3. SURFACE RECONSTRUCTION

According to the previously discussed data generation of the SLO technique, the recorded images also contain depth information beside the ordinary spatial 2D information. The degree of the reflected laser-light is encoded in gray-values of every pixel position - the higher the value (brighter) the stronger the reflectance and the nearer the surface boundary of the eye ground is located to the focus plane of the confocal laser beam.

The single images of the disparity corrected sequences are sorted according to the distance between the fundus and the focus plane of the confocal laser beam. The order of the sorted image sequences is defined with decreasing dioptrie values, i.e. from front to back beginning with the slice index no. 0 at the front. At each image position a 'depth-profile' P is derived out of the gray-values in order of the sorted image sequence. The depth profile P(x,y) at a fixed pixel position (x,y) is defined as the set of pixels (x,y,z) sorted by the z value or depth information:

$$P_{x,y} := \{ I(x, y, z_0), ..., I(x, y, z_{n-1}) \}$$

$$P_{x,y}(z) := I(x, y, z) \quad \text{with } z := z_0, ..., z_{n-1}.$$

I (x,y,z) is the intensity or the brightness at the position (x,y,z) and n is the number of slices of a SLO image sequence. While the brightness value of a pixel position (x,y) also encodes the depth of the surface boundary, the position of the maximal brightness value within this profile is determined.

Let  $P_{x,y}$  be the profile at the fixed image position (x,y) and z be the slice index, then the brightness maximum  $z_{max}(x,y)$ 

at the position (x,y) is defined as:

$$z_{\text{max}}(x,y): P_{x,y}(z_{\text{max}}) \geq P_{x,y}(z_i)$$

for all i := 0, ..., n-1

According to this definition,  $z_{\text{max}}$  is the slice index of that slice at a certain pixel position (x,y) where the highest brightness value is found and the surface boundary is estimated. The depth of this determined slice index is defined by the applied focus depth of the used confocal laser beam and therefore the surface boundary can be estimated out of it. Figure 6 illustrates the described proceeding of computing the surface boundary at image positions along an arbitrary column x.

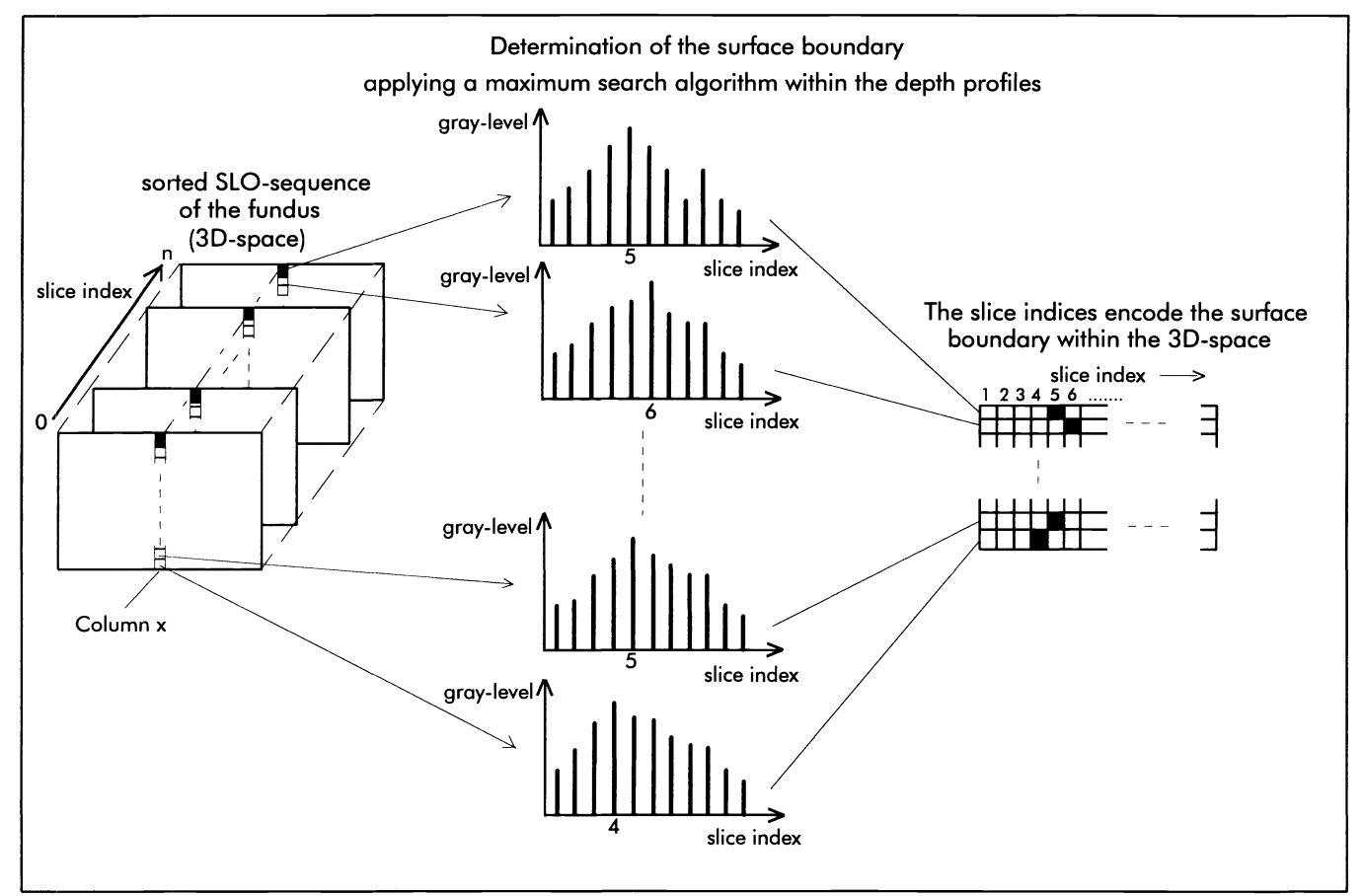


Fig. 6: Principle of surface reconstruction showed at an arbitrary column x. For each image position within a column, the surface boundary is computed out of the gray-levels of the sorted SLO sequence. The maximum position in each profile addresses the slice index, where the highest degree of reflection is measured and therefore, the boundary of the eye ground structure at the considered image position is estimated. The depth of the searched boundary is directly coupled with the slice index of the brightness maximum, e.g. slice index no. 5 for the first pixel in the illustrated column.

The whole surface information of the investigated eye ground area within the 3D space of the SLO sequence is finally represented only by the depth information of the detected slice indices. Determining the surface boundary for each pixel position of a SLO image sequence a first raw range image can be generated (Fig. 7).

Within these raw range images, the depth information is encoded in the gray-levels, so that deep locations will appear dark and higher ones bright. This raw surface representation shows some surface defects, appearing as extreme gray-level changes. These strong vacillations of the surface result from disturbances, like noise or diffuse reflections, occurring during the recording of the image sequence. The disturbances may cause an absolute maximum within the depth profile at a wrong profile position. This 'wrong' maximum may exceed the brightness value of the profile position, where the surface boundary would be expected (Fig. 8). During a first raw reconstruction step, this 'wrong' or disturbed surface information may cause peaks in the range image within almost homogeneous areas (Fig. 7).

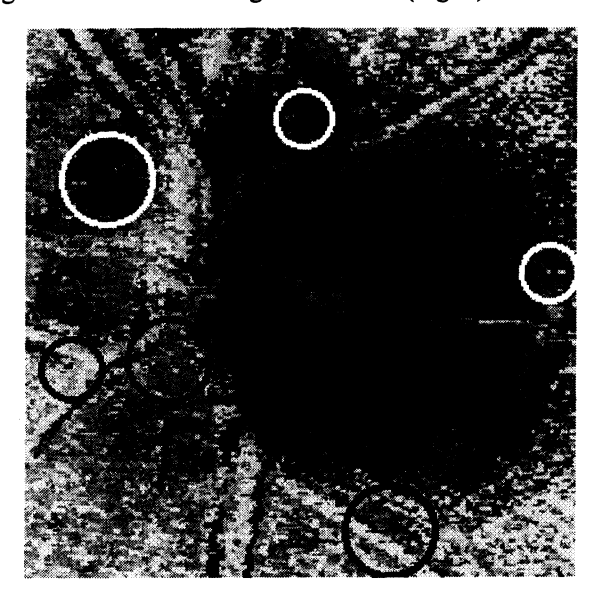


Fig. 7:

Visualization of the first raw reconstructed papilla surface as range image. Bright areas represent higher structures and dark intensity values deep structures. The circles mark samples of occurring defects within an almost homogeneous environment computed during a first raw reconstruction step. The black circles show samples of depth peaks, the white circles samples of height peaks.

Two kinds of defects appear, in the following called as height peaks and depth peaks. Height peaks in a range image represent small high, (bright) range structures within deep, dark regions. Whereas depth peaks are the opposite case, deep, dark structures within high, bright regions.

While the whole surface information can not be derived out of the profile position of the absolute brightness maximum in any case, an improvement algorithm which replaces the wrong depth information is developed. In order to remove these defects during further processing steps, it is necessary to look for alternative slice indices in the depth profile at the expected boundary position. In cases of disturbed surface information the expected surface boundary is often represented by a secondary local maximum in the depth profile.

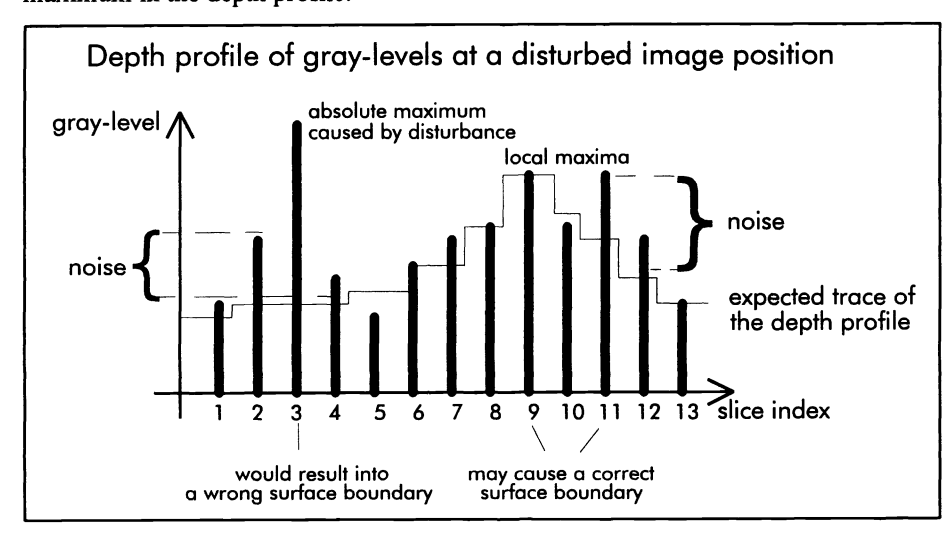


Fig. 8:
Synthetic depth profile illustrating the occurring disturbances, which cause deviations from an expected depth profile (second and third vertical bar). The disturbances of the whole image generation system may cause unexpected maxima at arbitrary locations, which may be higher than that of the expected depth position of the surface boundary.

# 4. ITERATIVE IMPROVEMENT OF THE SURFACE INFORMATION

The detected surface defects result from the depth information of the slice indices at unexpected absolute maximum positions within the depth profiles. To remove these surface defects it is necessary to choose alternative depth positions, i.e., slice indices, out of the depth profile which may replace the disturbed ones and may generate a defect free surface. The method of removing the detected surface defects is based on a set of alternative slice indices, which are derived from the investigation of other local maximum positions within the depth profile. The underlying assumption for this proceeding is, that the expected surface boundaries are already marked by a local brightness maximum, even in cases in which the absolute brightness maximum is caused by the mentioned disturbances. Therefore, a set of possible slice indices at one image position is determined out of all the local maxima which are detectable in the depth profile (Fig. 9).

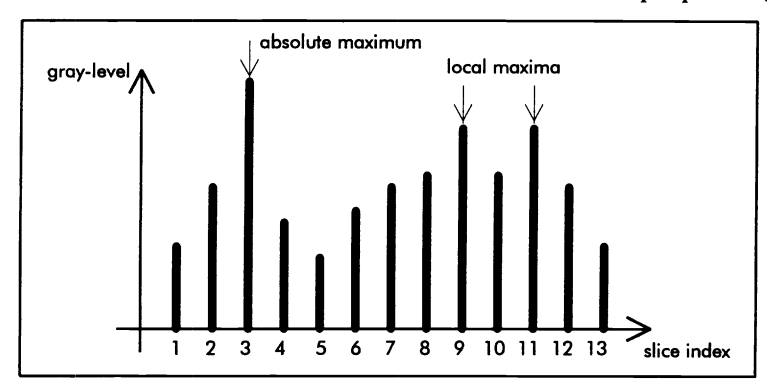


Fig. 9:

Synthetic example of a depth profile at a fixed image position with three local maximum positions of alternative surface candidates. The resulting index set consists of the slice indices no. 3, 9 and 11. The absolute brightness maximum is detected at an unexpected depth position at slice index no. 3. The slice index of the absolute maximum is only used to represent the surface boundary, during the first, initial step of the reconstruction process but it might be replaced by an other index during the improvement process.

In order to improve the homogeneity of the surface, we define a local homogeneity criterion, which is used to detect and to decide with which candidate a surface defect will be correct. This criterion is defined as the mean value d of the absolute differences of the actual slice index z at a local NxN environment of the considered surface position (x,y):

$$d(x,y) = \frac{1}{N^2 - 1} \sum_{i=x-m}^{x+m} \sum_{j=y-m}^{y+m} |z(i,j) - z(x,y)|, \text{ with } m = \frac{N-1}{2}$$

The smaller the value d is, the more homogeneous is the local surface environment considering the depth information of the investigated slice index at this pixel position. This mean value d is calculated at each image position for all the selected slice indices of the previously determined index set. The presented improvement process is still initialized with the absolute maximum because it results from the ordinary assumption of the reflection properties of the confocal laser beam within the fundus as mentioned above. To improve the surface boundary, the slice index yielding the smallest value of d is chosen (Fig. 10).

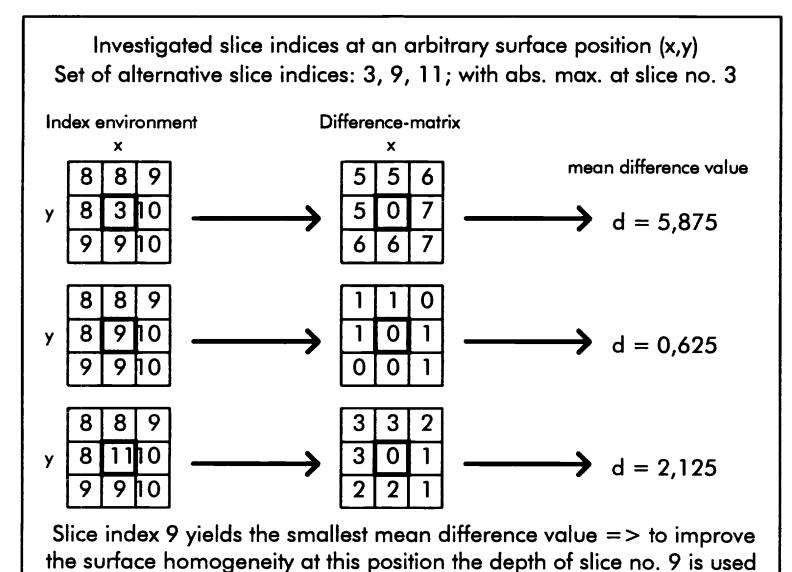
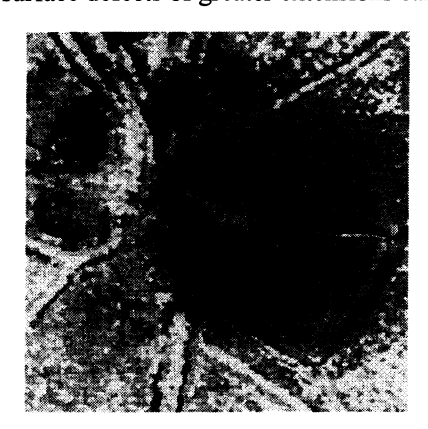


Fig. 10:

Surface improvement at the position (x, y) applied to a 3x3 environment to calculate the homogeneity criterion. The initial depth information of slice index no. 3 is replaced with the depth information of slice index no. 9 at this pixel position because the mean difference value d is minimal using the depth information of slice no. 9. This computation is applied to each pixel position in every iteration step. This improvement process yields stepwise an enhanced surface homogeneity within a growing environment.

The previously calculated depth information is replaced with this improved boundary candidate. Before exchanging the singular depth values, all the improvements are completely determined for the whole image, to achieve a direction invariant proceeding. This proceeding may correct defects of an extend of only singular pixels, i.e. defects in form of height peaks as well as of depth peaks. Since surface defects do not only occur as singular peaks, but also in extensions of up to twelve pixels (Fig. 7), they cannot be removed within one improvement step. Therefore, it is necessary to iterate the improvement process on the previously calculated, firstly improved surface information. Applying several iterations of the presented replacement process, surface defects of greater extensions can be removed stepwise (Fig. 11).



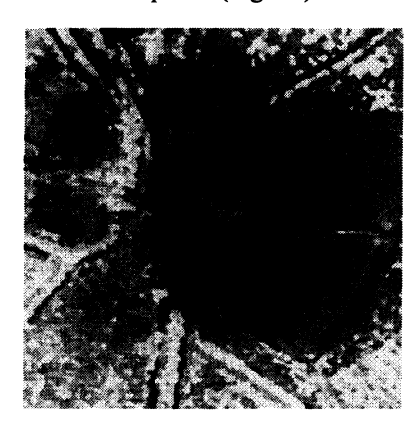




Fig. 11: Iterative improvement of the surface information. The three presented range images (from left to right) show the several results of the improvement steps after the first, second and third iteration. A replacement-tolerance of two depth units is used. During each iteration larger defects will shrink more and more, until they disappear. Each iteration achieves a visible improved homogeneity of the surface and the mean of the amount of changes of the depth information in each iteration decreases in about 50%.

## 5. OPTIMIZATION OF THE ITERATIVE SURFACE RECONSTRUCTION

# 5.1. Replacement-Tolerance

The previously described iterative improvement process removes nearly all surface defects. Replacing the current surface information with senseful alternative candidates, the surface defects are locally smoothed. This process may also affect already existing, real surface structures, like vessels or surface gradients, especially small ones. Therefore, the homogeneity criterion has to be restricted, in order to preserve little surface changes of real eye ground structures. This is accomplished by introducing a replacement-tolerance during the improvement process. The tolerance concerns the difference between the actual and the depth information of the calculated, improved surface boundary, before a replacement of the depth information is executed. If this difference is smaller or equal to the tolerance, no change is carried out. The rate of changes of the surface information is investigated, applying different replacement-tolerances during three iterations (Fig. 12).

Beginning at tolerances of two depth units, the rate of changes are significantly less in comparison to no tolerance, which improve the computing time. It can be seen, that replacement-tolerances of more than two depth units will preserve more real surface structures, but still remove the detected surface peaks (Fig. 13). An application of a tolerance of one depth unit does not enhance the reconstruction quality nor reduce the amount of changes.

	1. iteration	2. iteration	3. iteration
no tolerance	28.639	16.058	9.309
tolerance 1	22.380	10.843	5.888
tolerance 2	17.847	7.729	3.922
tolerance 3	14.363	5.796	2.888

Fig. 12: Statistics about the rate of changes while considering different replacement-tolerances within three iterative improvements steps of the raw range image shown in Figure 7. The change rates decrease rapidly applying replacement-tolerances greater one depth unit. Nearly no difference of the change rates can be observed between the replacement-tolerance of one depth unit and no tolerance. Improved surface conditions can be obtained using a tolerance of three depth units and two iterations compared to using no tolerance and only one iteration which needs the same effort of changes.





Fig. 13: Improved surface boundaries of Fig. 7 after three iterations without (left) and with a replacement-tolerance of three depth units (right). With the tolerance the resulting improved surface boundary exhibits more structure within homogenous regions. The surface improvement in both range images, however, is essentially the same, but with the tolerance, less surface information changes were necessary.

# 5.2. Recursive surface improvement

The proposed surface improvement method is realized as an algorithm, which is independent of the processing direction. This means, that the surface defects still exist during the processing from line to line and column to column, because the improvement method always considers the actual surface information. No replacement will be carried out at any surface position during the processing. Therefore, the surface positions with defects are still used during the calculation of the new surface boundaries of their neighboured positions. At these positions, the unchanged depth information might not always support a immediate removal of the surface defects and might not generate an appropriate homogeneous surface. A recursive calculation of the depth information would enhance the correction process. This means, that during the processing the old surface information is immediately replaced with the slice index of the improved one directly after its calculation. Therefore, the homogeneity criterion at the surface positions in the direct environment will be computed on the base of already improved values. This proceeding enhances the improvement process within only one iteration. In some cases the improvement process can already be stopped after the second iteration step, achieving comparable results as calculating three iterations using the non recursive proceeding. This direct replacement proceeding, however, is dependent on the processing direction, which may cause anomalies during the removal of surface defects. Therefore, this proceeding cannot be recommended in all cases, only if the computing time is a very important factor and small deviations of the reconstruction are acceptable.

## 5.3. Preprocessing of SLO slices

During the recording of a SLO sequence the occurring disturbances, as mentioned before, might appear as singular bright spots at unexpected but possibly random pixel positions within any SLO image of the sequence. In order to reduce the influence of these disturbances during the surface reconstruction, different smoothing filters are investigated as preprocessing application to eliminate or diminish these spots. The following smoothing filters are applied and investigated, the Butterworthlowpass [3], the Gauss and the mean filter as linear filters and the median, the k-trimmed-mean, the mid-range [11] and the outlier-filter [4, 7] as non-linear filters. The filters are applied only as preprocessing to each of the ordinary SLO images of the sequence before the surface reconstruction is accomplished. The reconstruction of the surface boundary out of the filtered SLO images reduces only the amount of small surface defects especially when using the non-linear filters. Therefore, less corrections within an iteration of a surface improvement have to be done which reduces the computing time. However, the surface reconstruction of previously filtered images exhibits the loss of small surface structures. The reason for this loss is, that a smoothing filter applied to the whole images as preprocessing is less sensible to fine structures than the introduced method of local smoothing, which only replaces possibly disturbed depth information with alternative ones at locations at which surface defects occur. Hence, a preprocessing by filtering the several recorded images is not useful to obtain an appropriate representation of the real eye ground structures.

## 6. RESULTS AND DISCUSSION

Applying the presented method to standard SLO sequences, a 3D reconstruction of the fundus can be achieved, which visualizes the volumetric properties of the Papilla and its morphologic structures. Utilizing the proposed improvement processes, nearly all occurred defects can be removed or at least are decreased in their size. The best results are obtained by considering a 3x3 environment to evaluate the homogeneity criterion and by iterating the improvement process three times. The number of replacements within a surface decreases rapidly with each iteration. The use of a replacement-tolerance of three or more depth units reduces remarkable the amount of changes and conserves more fine structures of the eye ground. The use of the replacement-tolerance realizes also a selective process, which changes only those depth information of surface positions, which have to be replaced. Only in cases of detecting a surface defect an appropriate alternative for an improved surface boundary is calculated. Therefore, the overall surface enhancement depends on several, selective, local improvement steps. The application of a tolerance value reduces the amount of changes and therefore the computing costs in each iteration. For example, the sum of the rate of changes of two iterations using the replacement-tolerance of three depth units is nearly equal to the rate of one iteration without considering a tolerance (Fig. 12). This means, within a given processing time, more improvements are possible if considering a tolerance than without.

A reduction of processing time for obtaining an improved surface boundary can also be achieved by applying the recursive replacement method. Using this proceeding, only two iterations may be necessary to obtain a comparable surface homogeneity as computing three non-recursive iterations. The calculated surface information, however, is dependent on the processing direction. The preprocessing of each SLO image applying the mentioned smoothing filters, before reconstructing the surface, reduces also the amount of surface defects and leads to less changes during an iteration. On the other hand, this proceeding finally diminishes the surface structure. Therefore, this preprocessing can not be used for a careful and exact surface reconstruction of the papilla.

The presented methods and the final 3D reconstruction of the derived depth information yet have not been applied and tested on a large amount of examples. A clinical application of the presented approach cannot be obtained at this stage of development. The methods might have to be modified in the case of routine examinations by oculists. An appropriate visualization tool has to be developed to present the computed reconstruction to oculists during routine examinations (Fig. 14). A complete medical examination tool might include more sophisticated features, like methods to extract the vessels in the fundus or to compute the geometrical structure of the papilla.

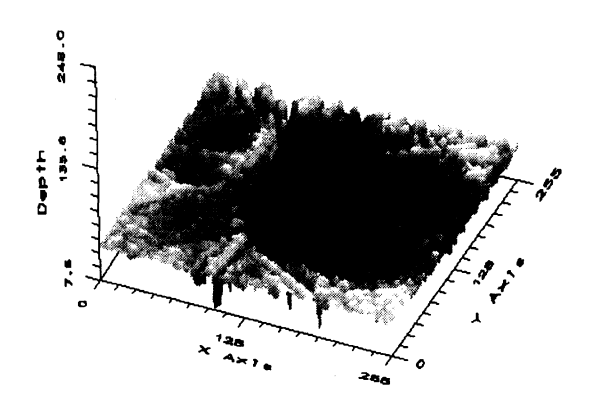


Fig. 14: 3D visualization of the resulting range image data of an examined SLO sequence

The presented approach shows some promising results to reconstruct and visualize the 3D information out of a sequence of SLO images. The developed algorithms are able to handle the occurring disturbances, while replacing only disturbed positions with senseful alternative depth information. Therefore, the existing fine structures of the eye ground can mostly be prevented from a raw detraction. A further development of a volumetric reconstruction tool for SLO images is possible and may be very useful, since it will help enhancing the diagnosis and the therapy of many diseases of the eye ground.

## REFERENCES

- [1] B. P. Bogert, M.J.R. Healy, J. W. Tukey, "The Quefrency Analysis of Time Series for Echoes: Cepstrum, Pseudo-Auto-covariance, Cross-Cepstrum and Saphe Cracking", In: Proceedings of the symposium on time series analysis, pp. 209-242, 1963
- [2] D. G. Childers, D. P. Skinner and R. C. Kemerait, "The Cepstrum: A Guide to Processing", In: Proceedings of the IEEE, Vol. 65, No. 10, pp. 1427-1443, Oct. 1977
- [3] R. C. Gonzalez, R. E. Woods, "Digital Image Processing", Addison Wesley Publishing Company, Inc., June 1992
- [4] J. S. Lim, "Two-dimensional signal and image processing", Prentice Hall, Englewood Cliffs, New Jersey, 1990
- [5] K.O. Ludwig, H. Neumann, B. Neumann, "Robust estimation of local stereoscopic depth", In: Förstner, Ruwiedel (eds.), Robust Computer Vision: Quality of Vision Algorithms, pp. 290-312, Wichmann, 1992
- [6] F. Offenhäuser, C. Zeiss, "Fundustopometrie mit dem Laserscanophthalmoskop", Sonderdruck aus dem "Jahrbuch für Augenheilkunde", pp. 181-186, Oberkochen, 1992
- [7] W. K. Pratt, "Digital Image Processing", Second Edition, , Wiley-Interscience Publication, John Wiley & Sons Inc., New York, 1991
- [8] J. Rosenthal, "Arterielle Hypertonie", Aetiopathogenese Diagnostik Therapie, Springer Verlag, Berlin, 1984
- [9] R. H. Webb, G. W. Hughes and F. C. Delori, "Confocal scanning laser ophthalmoscope", In.: Applied Optics, Vol. 26, No. 8, pp. 1492-1499, April 1987
- [10] Y. Yeshurun, E. L. Schwartz, "Cepstral Filtering on a Columnar Image Architecture: A Fast Algorithm for Binocular Stereo Segmentation", In: IEEE Transactions on Pattern Analysis and Machine Intelligence, Vol. 11, No. 7, pp. 759-767, June 1989
- [11] P. Zamperoni, "Methoden der digitalen Bildsignalverarbeitung", Vieweg, Braunschweig, 1991